

# A Content-Dependent Naturalness-Preserving Daltonization Method for Dichromatic and Anomalous Trichromatic Color Vision Deficiencies

Neda Milić

Department of Graphic Engineering and Design, Faculty of Technical Sciences, Novi Sad, Serbia  
E-mail: milicn@uns.ac.rs

Miklós Hoffmann and Tibor Tómacs

Eszterházy Károly College, Institute of Mathematics and Computer Science, Eger, Hungary

Dragoljub Novaković and Branko Milosavljević

Department of Graphic Engineering and Design, Faculty of Technical Sciences, Novi Sad, Serbia

**Abstract.** Color vision deficiency represents an inability to perceive differences between certain colors that can be distinguished in the case of regular color vision. This article proposes a new daltonization method for re-coloring image segments perceived as confusingly colored by color deficient observers and, thus, to improve their perceived image quality. The idea behind this approach is that only one image color center should be located on one confusion line. If colors of two or more segments lie on the same confusion line, then they should be remapped in a direction perpendicular to the confusion line taking into account the image content—the color distribution of other segments. The method conserves the image naturalness by restricting, for each segment center, an area of admissible remapping. This achieves re-coloring balance where colors are made sufficiently distinguishable from each other, but they do not deviate too much from the original image colors. The proposed re-coloring concept is applicable to all types of dichromacy and anomalous trichromacy with adjustment for their set of confusion lines. The simulation results show that the re-coloring converts an original image to a version with improved color distinction, confirmed by evaluations of eight color deficient users. An intentionally chosen example demonstrates when and why the proposed method performs better against content-independent methods. Furthermore, results and subjective evaluations indicate that the method provides more natural re-coloring results for anomalous trichromats than in the case of content-dependent methods optimized for dichromats.

© 2015 Society for Imaging Science and Technology.  
[DOI: 10.2352/J.ImagingSci.Technol.2015.59.1.010504]

## INTRODUCTION

Normal human color vision starts with the light absorption by color photoreceptors within the retina classified as  $L$ ,  $M$  and  $S$  cones, due to their highest sensitivities to long, middle and short wavelengths, respectively.<sup>1</sup> The triplet of cone responses is interpreted as a particular color sensation in the vision center, so people with normal color vision may be referred to as trichromats.<sup>1</sup>

A significant percentage of the human population (approximately 8% of males and 0.4% of females according to statistics for the Caucasian population<sup>2</sup>) has some form of color vision deficiency (CVD), manifested with difficulties in color recognition and differentiation.

The severity of this, predominantly genetic, condition depends on the number of distinctive cone signals. Hence, we can distinguish three main categories of CVD:<sup>3</sup> monochromacy as a condition of total color vision deficiency with two or all three cone types absent; dichromacy as partial color vision deficiency caused by the absence of one cone type (the  $L$  type in protanopia, the  $M$  type in deuteranopia and the  $S$  type in tritanopia); and anomalous trichromacy as moderate color vision deficiency where all photoreceptors are present, but one class has shifted sensitivity (the  $L$  type in protanomaly, the  $M$  type in deuteranomaly and the  $S$  type in tritanomaly). The sensitivity of protanomalous  $L$  cones shifts closer to that of regular  $M$  cones, while the peak sensitivities of the anomalous  $M$  and  $S$  types move toward longer wavelengths. The malfunction or absence of  $L$  and  $M$  cones causes over 99% of all CVD cases with the common name red–green color vision deficiency.<sup>3</sup> One-quarter of them are dichromats (protanopes and deuteranopes), while three-quarters are anomalous trichromats (protanomalous and deuteranomalous).

Considering the prevalence of color deficient users, it is important to optimize color information accessibility in digital content for them. The succeeding sections provide the theoretical basis of simulating anomalous color vision, the state-of-the-art in the image enhancement for color deficient viewers and the proposition of a new simple and computationally non-demanding re-coloring method that improves color distinction in image content for both dichromatic and anomalous trichromatic deficiencies while conserving naturalness.

## ANOMALOUS COLOR VISION

Although the spectral power distribution of light falling on the retina is a function of wavelength, all information about

Received Oct. 7, 2013; accepted for publication Mar. 11, 2015; published online Apr. 2, 2015. Associate Editor: Jon Yngve Hardeberg.  
1062-3701/2015/59(1)/010504/10/\$25.00

its spectral composition is lost after absorption.<sup>4,5</sup> We can model the cone responses as the following vector:<sup>4</sup>

$$[L, M, S] = \int [l(\lambda), m(\lambda), s(\lambda)]E(\lambda)d\lambda, \quad (1)$$

where  $E(\lambda)$  represents the spectral power distribution of a stimulus and  $l(\lambda), m(\lambda), s(\lambda)$  are the spectral sensitivity functions of the cone types. Therefore, any stimulus can be characterized as a point in a 3D human visual space, spanned by quantum catches of cone types.<sup>4</sup> Stimuli with different spectral compositions that plot at the same point will appear alike.<sup>5</sup> This specification of a stimulus approximates the color vision mechanism since the color appearance depends on further nonlinear processing of the cone responses.<sup>1,3</sup>

Compared with normal trichromatic vision, color deficiency implies reduction of color gamut manifested with a loss of hue discrimination. The nature of color deficient vision is relatively well understood thanks to the extensive reports of unilateral dichromats (subjects with one normal and one dichromatic eye). Reports determine invariant hues appearing the same to dichromats and standard observers:<sup>6</sup> achromatic stimuli for all CVD types, monochromatic stimuli of 475 nm (a blue hue) and 575 nm (a yellow hue) for protanopia and deuteranopia, and monochromatic stimuli of 485 nm (a blue-green hue) and 660 nm (a red hue) for tritanopia.

Several methods for simulating dichromacy exist on the basis of assumptions about invariant hues, where the method defined by Brettel et al.<sup>6</sup> and Vienot et al.<sup>7</sup> is most frequently used. They explain gamut mapping from trichromacy to dichromacy using *LMS* space in which the orthogonal axes represent cone responses. Figure 1 demonstrates mapping of a color stimulus to a dichromatic gamut. For each type of dichromacy, a reduced color gamut is presented with two half-planes divided by the achromatic axis and anchored on points specifying the invariant stimuli.<sup>6</sup>

Dichromats confuse colors that differ only in the intensity of the absent cone response<sup>8</sup> (the Ishihara test uses this fact). The dichromatic version of a given color stimulus  $C$  is found as a projection to a particular half-plane in the direction parallel to the missing cone response:  $CC_p \parallel L$  axis,  $CC_d \parallel M$  axis and  $CC_t \parallel S$  axis. Lines  $CC_p, CC_d$  and  $CC_t$  are called confusion lines since the points that lie on them are perceived as the same color by individuals with the corresponding dichromacy.

The value of the missing response is calculated from two existing ones that remain unchanged:<sup>6</sup>

$$\begin{aligned} C_P &= \left( -\frac{bM + cS}{a}, M, S \right), & C_D &= \left( L, -\frac{aL + cS}{b}, S \right), \\ C_T &= \left( L, M, -\frac{aL + bM}{c} \right), \end{aligned} \quad (2)$$

where the  $a, b$  and  $c$  coefficients are obtained from the *LMS* values of stimulus  $E$  (dichromatic white point) and the nearest invariant monochromatic stimulus  $A$  in the following

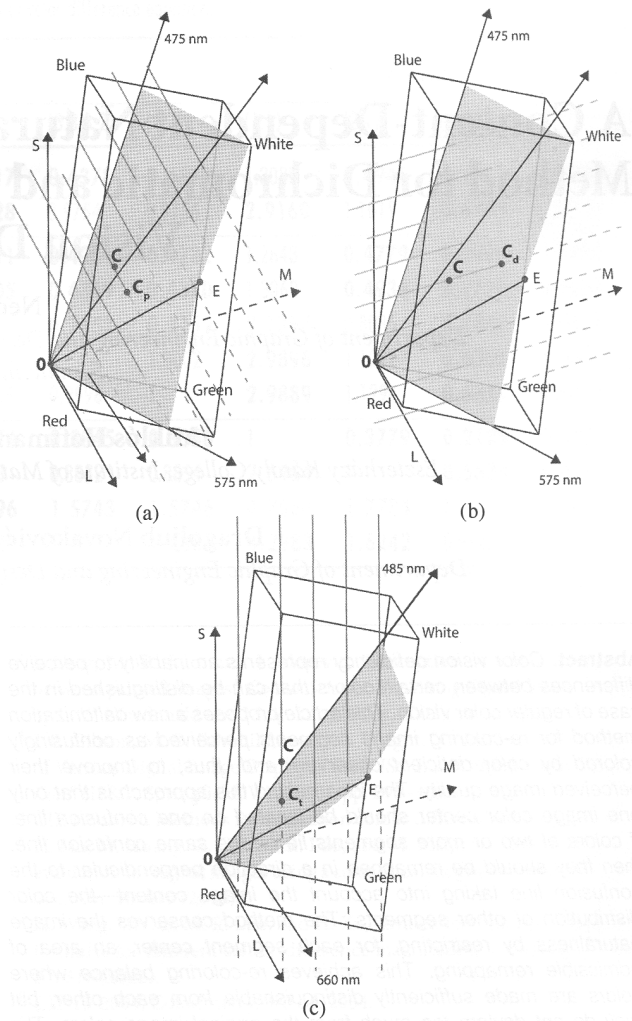


Figure 1. Projection of a color to a dichromatic gamut (gray half-planes) in *LMS* space. The dichromatic version of a given stimulus  $C$  is projected to a particular half-plane in the direction parallel to the missing cone response:<sup>6</sup> (a) protanopia ( $CC_p \parallel L$  axis), (b) deuteranopia ( $CC_d \parallel M$  axis), (c) tritanopia ( $CC_t \parallel S$  axis).

manner:<sup>6</sup>

$$\begin{aligned} a &= M_E S_A - S_E M_A, & b &= S_E L_A - L_E S_A, \\ c &= L_E M_A - M_E L_A. \end{aligned}$$

When confusion lines are converted from *LMS* color space (Fig. 1) to the perceptually uniform CIE 1976  $u'v'$  chromaticity diagram (Figure 2), they are no longer parallel—they converge to a specific confusion point. Excluding the lightness dimension, the dichromatic chromaticity gamut is represented by the line connecting two invariant monochromatic stimuli on the edge of the locus. The dichromatic perception of a given chromaticity  $C$  is found as an intersection of the confusion line and the gamut line for each type of dichromacy (see Fig. 2).

Unlike dichromats, anomalous trichromats have three distinctive cone responses. Since the spectral sensitivity shift of the malfunctioning cone type can differ, the mapping normal to the anomalous trichromatic gamut is not universal—it covers a broad variety of almost normal

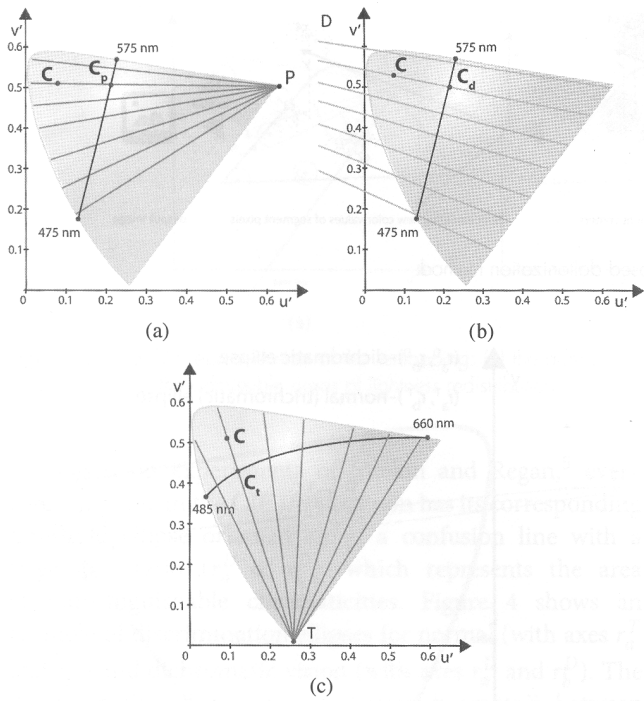


Figure 2. Projection of a color to a dichromatic chromaticity gamut in the CIE  $u'v'$  diagram.<sup>5</sup> The dichromatic perception of a given chromaticity  $C$  is found as an intersection of the confusion line and the gamut line. Confusion lines converge to a specific confusion point: (a) for protanopia  $P(0.68, 0.50)$ , (b) for deuteranopia  $D(-1.22, 0.78)$ , (c) for tritanopia  $T(0.26, 0.00)$ .

to significantly reduced gamut such as that exhibited by dichromats. Machado et al.<sup>3</sup> define simulation models of anomalous trichromatic CVD based on the stage theory of human color vision.<sup>3</sup> Simulated RGB values are given by a single matrix multiplication  $\phi_{CVD}$ :<sup>3</sup>

$$\begin{bmatrix} R_{CVD} \\ G_{CVD} \\ B_{CVD} \end{bmatrix} = \phi_{CVD} \begin{bmatrix} R \\ G \\ B \end{bmatrix} = \Gamma_{\text{normal}}^{-1} \Gamma_{CVD} \begin{bmatrix} R \\ G \\ B \end{bmatrix}, \quad (3)$$

where  $\Gamma$  represents a class of transformation matrices that map the RGB values to the opponent channels—one achromatic channel, light–dark ( $WS$ ), and two chromatic channels, red–green ( $RG$ ) and yellow–blue ( $YB$ ):<sup>3</sup>

$$\begin{bmatrix} WS \\ YB \\ RG \end{bmatrix} = \Gamma \begin{bmatrix} R \\ G \\ B \end{bmatrix} = \begin{bmatrix} WS_R & WS_G & WS_B \\ YB_R & YB_G & YB_B \\ RG_R & RG_G & RG_B \end{bmatrix} \begin{bmatrix} R \\ G \\ B \end{bmatrix}. \quad (4)$$

When protanomalous and deuteranomalous cones have a spectral shift of approximately 20 nm, the color perception is close to that of protanopes and deuteranopes by Brettel and Vienot’s method.<sup>3</sup>

**DALTONIZATION METHODS**

Simulation of CVD enables us to see the image content from the perspective of a color deficient individual. Several software solutions for simulating CVD (mostly of dichromatic type) are available online, like Vischeck,<sup>9</sup> Visolve<sup>10</sup> and a

Google Chrome extension (Chrome Daltonize),<sup>11</sup> or offline, like the plug-in for Adobe InDesign software.<sup>12</sup>

Based on well-established simulation methods,<sup>3,6,7,13–15</sup> some guidelines on web accessibility are defined<sup>16–18</sup> which solve problems concerning the choice of color scheme for design in documents, software interfaces, web presentations, etc. However, they have limited use in the case of natural images.

Therefore, in addition to guidelines, simulation results can be used for defining a re-coloring method that adapts the image content so that individuals with CVD can see the content as similarly as possible to an average observer. This color adaptation, commonly called daltonization, is a complex and still active problem of mapping the image gamut to a reduced one. Daltonization methods can be divided into two categories: content independent and content dependent.

Content-independent methods do not assure color differentiation by a CVD observer because they use a global pixel-based processing that does not take into account the image content or spatial distribution of confusing colors.<sup>9,11,19–26</sup> The entire image is treated in a uniform manner, and the resulting pixel value is a function of its original value, regardless of its location or other pixel values. It often happens that re-coloring solves the initial problem but creates a new confusing pair between the new (remapped) color and the color of another neighboring area. Also, colors that are initially clearly distinctive can be remapped into indistinguishable combinations. Many of these simple methods are implemented in the web environment and modify HTML pages on a pixel basis.<sup>11,19,26</sup>

A frequently used solution for solving color accessibility in the web environment, the Chrome Daltonization extension,<sup>11</sup> is based on the simple content-independent algorithm defined by Fidaner et al.<sup>24</sup> The plug-in uses an error matrix obtained by subtracting simulated dichromatic values from the original RGB values and recalculates new pixel values by adding components of the error matrix multiplied by weighting coefficients to initial values.<sup>24</sup>

A specific case of a content-independent algorithm is the most current spectral-based method by Kotera.<sup>25,26</sup> The nature of this re-coloring which uses the projection of spectral data to the dichromatic cone response space is content independent since one pixel’s color always remaps into the same color. The fundamental spectral data are captured from the RGB values by a pseudo-inverse projection, and the lost spectra are calculated as the difference between fundamental spectra visible to trichromats and dichromats. The method aims to maximize the spectral visibility for dichromats by adding the lost spectra to the fundamental spectra of the initial image.<sup>26</sup>

The content-dependent category includes histogram-based, neighborhood-based, region-based and other methods where the final pixel color value depends on the initial image gamut, histogram or location of the pixel. These methods are more complex and computationally demanding,<sup>27–34</sup> but provide more successful differentiation of colored elements using the benefits of genetic

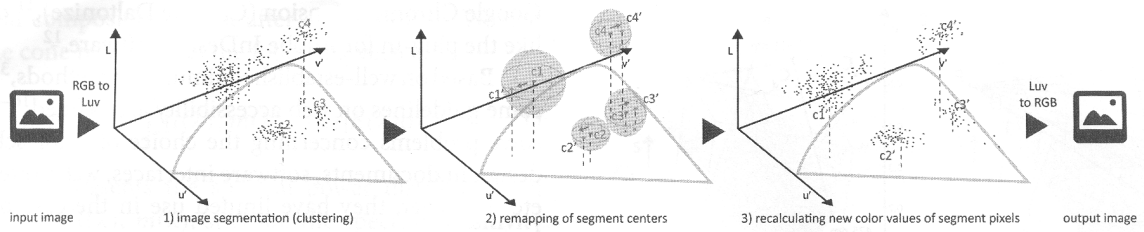


Figure 3. The steps of the proposed daltonization method.

algorithms,<sup>27,28</sup> mass-spring optimization,<sup>29</sup> affine transformations,<sup>30</sup> neural networks,<sup>31</sup> etc. However, there are problems with the conservation of image naturalness and color identification, as users can now distinguish between all the colored elements, but colors are often remapped to completely different ones, and that presents problems in the case of real-life images. Many content-dependent methods aim to adapt images optimally for dichromatic CVD (e.g., Machado’s method<sup>33</sup>), where the resulting image has an exaggeratedly reduced gamut for moderately anomalous trichromats with almost normal hue discrimination.

**METHOD**

**Motivation**

There is still an open search for an “ideal” re-coloring method to adapt image content in an optimal way for all groups of color deficient users. The proposed content-dependent approach tries to overcome the limitations of the content-independent methods, but preserve their computational simplicity. It also aims to utilize a uniform remapping concept for every type and severity of color deficiency, unlike content-dependent methods optimized for dichromats. By restricting the area of admissible remapping for each segment center, the method achieves re-coloring balance between increasing color contrast and conserving the naturalness for CVD users, meaning that the resulting colors will not deviate too much from the original image colors (colors the users are accustomed to seeing in real life).

**The Algorithm Steps**

The proposed daltonization method includes the following steps, which are graphically presented in Figure 3.

1. Image segmentation based on chromaticity and defining centers as representative colors of each segment. The clustering is based on the Euclidean distance metric in the  $Lu'v'$  space between chromaticity values excluding the variations in lightness. K-means clustering<sup>34</sup> segments groups of pixels based on their location in the  $u'v'$  plane in a manner such that the pixels within each cluster are as close to each other as possible, and as far as possible from pixels in other clusters.<sup>35</sup> A representative color center is then selected for each segment by averaging all colors in it.
2. Remapping of color centers in a direction perpendicular to the confusion line inside the corresponding admissible area. The basic idea is simple—if the color centers of two image segments lie on the same confusion line, then

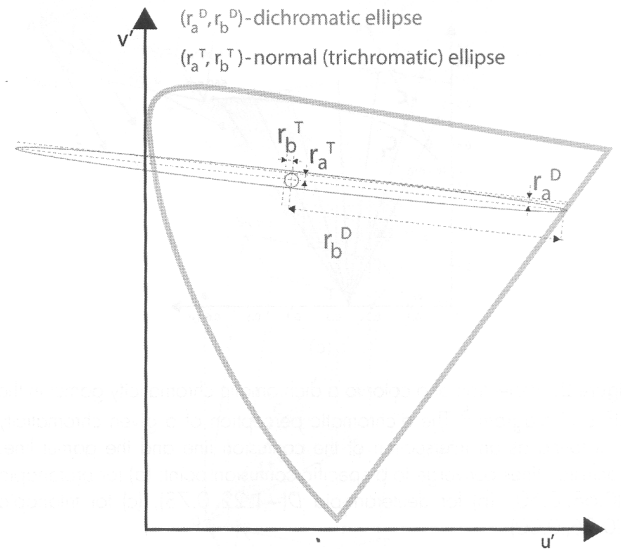


Figure 4. An example of threshold areas for normal and dichromatic color vision in the CIE  $u'v'$  chromaticity diagram.

they should be remapped in a direction perpendicular to the confusion line (rotation around the confusion point). The resulting positions of the color centers are content dependent: they depend on the number of segments, the initial positions of segment centers and the defined admissible area.

3. Replacing the original color centers with the new ones and recalculating the color values of other pixels in segments.

The differences in color values ( $\Delta u'$ ,  $\Delta v'$ ,  $\Delta L$ ) between every re-colored pixel in the segment and the remapped center of the segment are the same as before remapping (with the exception of clipped values that were remapped outside the possible gamut).

The CIE  $Lu'v'$  color space is chosen for the re-coloring environment because of its perceptual uniformity—equal distances in space correspond moderately well to equal perceptual differences and, thus, it is a good tool for the computation of perception thresholds.<sup>5</sup> Since the human eye has limited accuracy, there is a region on the chromaticity diagram, i.e., the MacAdam ellipse, that contains colors indistinguishable from the color at the ellipse center.<sup>36</sup> While the size and orientation of the discrimination ellipses in the CIE  $xy$  diagram vary widely depending on the position of a chosen color, in the CIE  $u'v'$  diagram the ellipses of normal color distinction are nearly circular.<sup>13</sup>

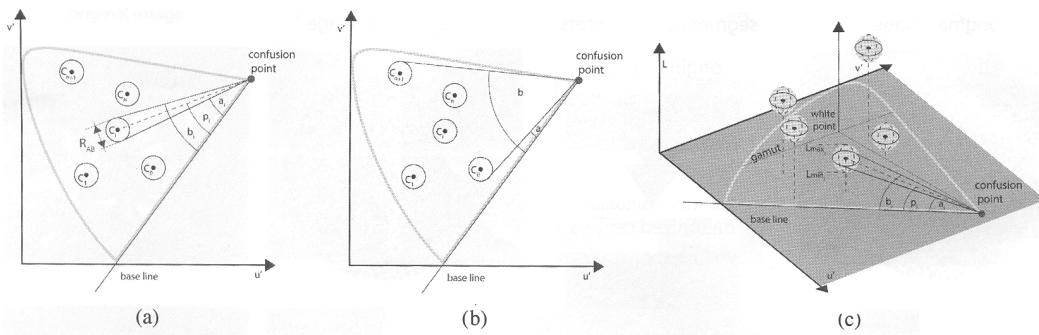


Figure 5. Graphic representation of the remapping: (a) the admissible area of one segment, (b) the fixed leftmost and rightmost positions in the set of color centers, (c) the admissible areas of lightness redistribution.

Based on experiments of Mollon and Regan,<sup>5</sup> every confusion line in the CIE  $u'v'$  diagram has its corresponding threshold ellipse oriented along a confusion line with a large axis ratio ( $r_a^D \ll r_b^D$ ), which represents the area of indistinguishable chromaticities. Figure 4 shows an example of discrimination ellipses for normal (with axes  $r_a^T$  and  $r_b^T$ ) and dichromatic vision (with axes  $r_a^D$  and  $r_b^D$ ). The discrimination ellipses of anomalous trichromats lie between these extremes ( $r_a^T < r_a^{AT} < r_a^D$  and  $r_b^T < r_b^{AT} < r_b^D$ ). The  $r_b^{AT}$  axis should be taken to indicate the quantitative measure of the subject's color deficiency.

Each type of CVD has a different set of confusion lines, whereas the remapping concept remains the same.

### Remapping Color Centers

Figure 5 shows the concept of the remapping algorithm. The color points  $c_0, c_1, \dots, c_i, \dots, c_n, c_{n+1}$  represent color centers of image segments. For each point, there is a corresponding admissible area, an ellipse oriented along the confusion line, where it is allowed to remap the point. In the case of dichromacy, the axis of the admissible area in the direction of the confusion line is irrelevant for remapping, while the axis perpendicular to the confusion line is relevant for the calculation and it must be larger than the minor axis of the discrimination ellipse ( $R^{AB} > r_a^D$ ). For less severe anomalous trichromatic deficiencies, the admission areas could be smaller. The line connecting the position of the color point  $c_i$  and the confusion point (dashed line, Fig. 5(a)) and the lines connecting the extreme admissible positions of the color point  $c_i$  and the confusion point (two thick lines, Fig. 5(a)) form with the baseline three angles denoted by  $p_i, a_i$  and  $b_i$ . In this case, the baseline approximates the leftmost confusion line, but it can be any line that fulfills the condition that all admissible areas are on one side of the line. The aim is to redistribute these colors in such a way that the lines from the confusion point to the color points are as far from each other as possible, or, in other words, to find the angles  $p_i$  distributed within the admissible intervals in the most even way possible.

With  $a_i$  and  $b_i$  predetermined for the color  $c_i$ , the aim is to change  $p_i$  ( $p_i \in [a_i, b_i]$ ) in order to find the optimal angle—the optimal position of the color point  $c_i$ .

The set of color positions can be compared with a model in which points  $c_i, i = 0, 1, \dots, n + 1$ , represent positions of electrons or small magnets and due to their magnetic charge they want to be pushed as far as possible from each other, but their individual intervals restrict their movement. If we make the analogy between the confusion point and the atom nucleus, and between a confusion ellipse and an orbital in which the presence of two or more electrons induces repulsive forces between them, then color points, like electrons, should inhabit different orbitals to minimize the repulsions between electrons and make the atom more stable. The analogy can also be made between the order rule of filling orbitals and the admissible area where an electron can jump only to a neighboring orbital and not to a distant one. This model tends to seek the equilibrium state. For that purpose, the first color is fixed at the leftmost position,  $p_0 = a_0 = a$ , and the last color is fixed at the rightmost position,  $p_{n+1} = b_{n+1} = b$ , while other color points are iteratively moved (Fig. 5(b)). Inside a large interval  $[a, b]$  are placed smaller subintervals  $[a_i, b_i]$  in ascending order ( $a < a_1 < a_2 < \dots < a_n, b_1 < b_2 < \dots < b_n < b$ , and  $a_i < b_i$  for  $i = 1, \dots, n$ ) which can overlap. The simple mathematical problem is formulated as follows:

$$p_i = \begin{cases} \frac{1}{2}(p_{i-1} + p_{i+1}), & \text{if } a_i < \frac{1}{2}(p_{i-1} + p_{i+1}) < b_i, \\ a_i, & \text{if } \frac{1}{2}(p_{i-1} + p_{i+1}) \leq a_i, \\ b_i, & \text{if } b_i \leq \frac{1}{2}(p_{i-1} + p_{i+1}), \end{cases} \quad (5)$$

where  $p_1, p_2, \dots, p_n$  are positive real numbers in ascending order  $p_1 \leq p_2 \leq \dots \leq p_n$ . Then the point system  $\{p_1, \dots, p_n\}$  is called stable with respect to the set of color points.

The restriction of areas admissible for remapping and the maintenance of the original angle sequence after remapping conserve the image naturalness. Re-coloring aims to achieve balance, where colors will render sufficiently distinguishable from one another for a color deficient observer, but they will not deviate too much from the original image colors.

A requirement for the color centers to be distinguishable from each other for a particular CVD type is that each pair of centers lies outside the contour of the corresponding discrimination ellipse. However, when too many color centers are concentrated in the same area of the chromaticity diagram

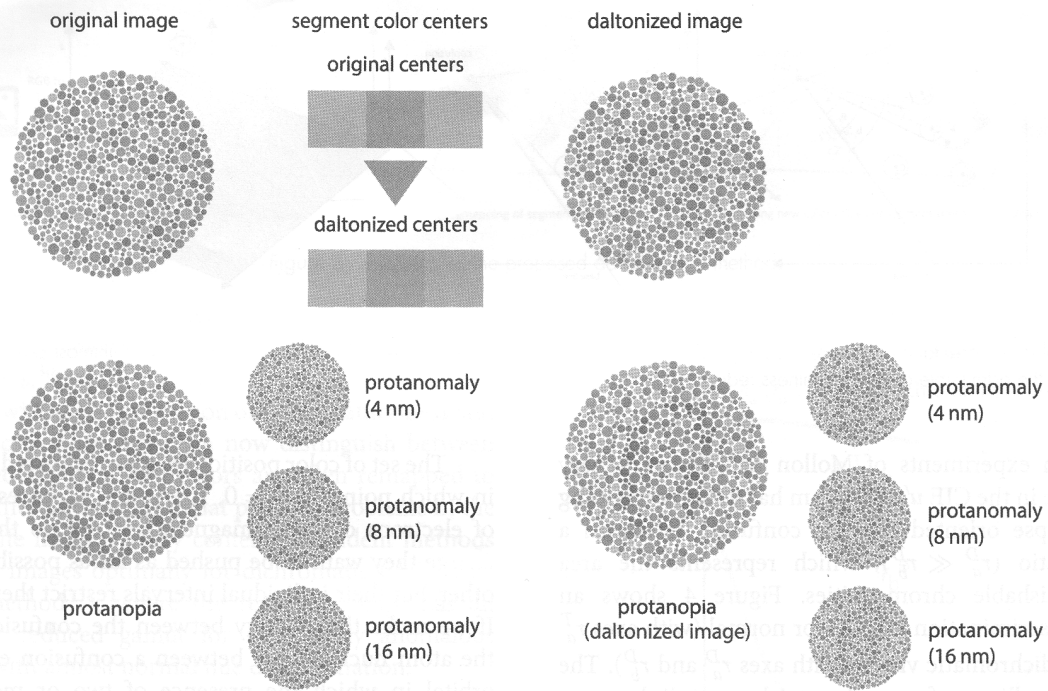


Figure 6. The daltonization results for protanopia and protanomaly obtained with the new method for an Ishihara plate.

for the initial image or when there are too many image segments in general, this requirement can be hard to achieve.

Enlargement of the admissible area  $[a_i, b_i]$  can provide a satisfying re-coloring solution for situations when more color centers are placed near same confusion line, although it reduces image naturalness. When there are too many color centers then adjusting the admissible area cannot make the difference, and it is convenient for the lightness value to be included in the remapping (Fig. 5(c)). Redistribution of the color centers in the direction of the lightness axis optimizes the daltonization. The lightness remapping should be applied separately for the blue and yellow parts of the dichromatic gamut line since colors projected on opposing parts of the dichromatic gamut line have a satisfying distinction in chromaticity.

### Objective and Subjective Evaluation

The simulation of dichromatic image versions was accomplished with the Chrome Simulation filter<sup>11</sup> using a simplified Vienot and Brettel method,<sup>7</sup> while anomalous trichromatic versions were obtained using Machado's method.<sup>3</sup> The re-coloring results were obtained for the cases of anomalous trichromacy with spectral sensitivity shifts of anomalous cones of 4, 8 and 16 nm.

Apart from objective computer simulation, the daltonization results were evaluated by eight color deficient users with different types and severities of red-green color deficiency: one protanope, four protanomalous and three deuteranomalous. They evaluated the perceived image quality obtained with the new daltonization method in comparison to original images and daltonization results of other methods.

### RESULTS AND DISCUSSION

To demonstrate the efficiency of the new method, simple and frequently used examples—an Ishihara plate and a natural image with a red-green confusing combination—were used. The computer simulations of the original image and the re-colored result along with their corresponding color centers are shown for the Ishihara plate in Figure 6 and for the natural image in Figure 7. The Ishihara plate is segmented into three regions while the natural image has four segments. For the daltonization procedure an admissible remapping angle of  $p_i - a_i = b_i - p_i = 4^\circ$  was used.

The protanope and protanomalous versions of the daltonized image simulation show that the segments are made sufficiently distinguishable from each other for the CVD users, and this was confirmed by the subjective evaluation of all eight subjects including the deuteranomalous observers. An additional advantage, confirmed by the CVD observers, is that the natural image remains quite natural to the CVD observers—the colors remain quite close to the ones that they are used to.

Apart from the examples in Figs. 6 and 7, frequently used for solving the color distinction problem with daltonization, a more complex metro map with five color centers was chosen for showing the comparative benefits of the new method against state-of-the-art content-independent methods: the one used in the Chrome Daltonization<sup>11</sup> extension for solving the color-accessibility issue in the web environment and a recently published spectral-based daltonization.<sup>26</sup>

The comparison results on the metro map are shown in Figure 8. The hexadecimal values of the color points on the map are (Fig. 8(a)): M1(#9b9b23), M2(#49a523),

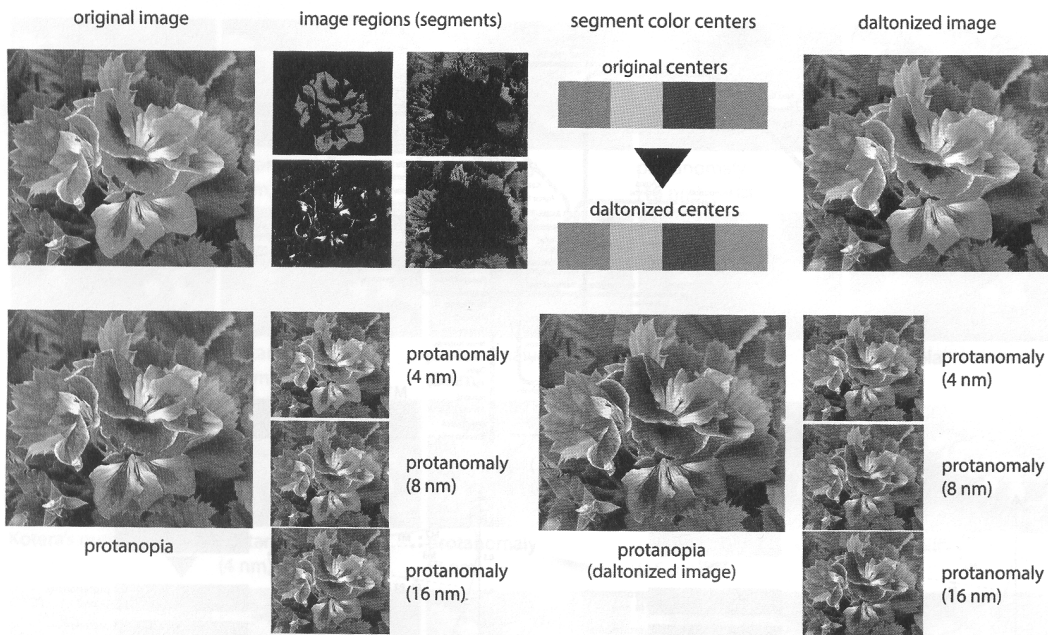


Figure 7. The daltonization results for protanopia and protanomaly obtained with the new method for a natural image with a red–green confusing combination.

M3(#64e371), P1(#5a70bb) and P2(#9f195a). Fig. 8(b) presents the original map with one problematic color pair, M1 and M2 (which lie on the same confusion line), for individuals with protanopia. For the daltonization procedure an admissible remapping angle of  $p_i - a_i = b_i - p_i = 5^\circ$  was used.

The image adaptation conveyed with Chrome Daltonize solves this problematic combination but creates two new ones—between the M1 and M3 segments, and between the P1 and P2 segments (Fig. 8(c)).

In the case of Kotera’s daltonization method (Fig. 8(d)), the P2 center is remapped to the opponent part of the dichromatic chromaticity line and now lies on the same confusion line as the remapped M2 center, although there is a distinction between them due to the difference in lightness. The Kotera remapping result creates confusion in color information coding since the P2 region is now visually closer to the M group of transportation routes. The final scheme has reduced chromaticity diversity in comparison to the original one.

The example demonstrates that a fixed content-independent transformation does not work correctly for any image, because it could happen that colors that are difficult to distinguish remain confusing after daltonization. Even worse, colors that were clearly distinctive can be remapped into indistinguishable combinations, like in Fig. 8(c).

The content-dependent method defined by Machado et al.<sup>33</sup> and optimized for dichromatic CVD was also used for comparison. Machado’s method gives a good result concerning color distinction (Fig. 8(e)). However, the appearance of the daltonized image is the same for dichromatic and anomalous trichromatic CVD users, meaning that the image gamut is reduced far more than

necessary for anomalous trichromats. The observers with anomalous trichromacy commented on this as an unwanted result, especially two of them with color discrimination close to normal color vision.

The new method redistributes segment centers evenly without making new indistinguishable color pairs—only one color center is placed on each confusion line (Fig. 8(f)), while remapped color centers do not deviate too much from the original colors. The daltonization result gains in both the total number of distinctive colors and the global chromaticity diversity. The obtained color distinction is emphasized, including the remapping in lightness dimension (Fig. 8(g)).

While Kotera’s and Machado’s methods minimize the difference in perception of the daltonized image between normal and dichromatic vision, resulting in reduction of image gamut for standard observers, the new approach aims to keep the image perception for each user close to their perception of the original image. This concept has justification in the fact that image content in the digital environment can be adapted (personalized) on request, rather than applied in one version for all. Six anomalous trichromatic users marked the color scheme obtained with the new method (Fig. 8(f)) as the choice of preference among all versions. A protanope user picked the new daltonization method with lightness remapping included as the scheme with the best color distinction (Fig. 8(g)), while one deuteranomalous user preferred the Machado daltonization result.

Figure 9 presents daltonization results for a natural image with large image gamut. This type of image content can indicate shortcomings in the daltonization algorithm that cannot be discovered using conventional examples with

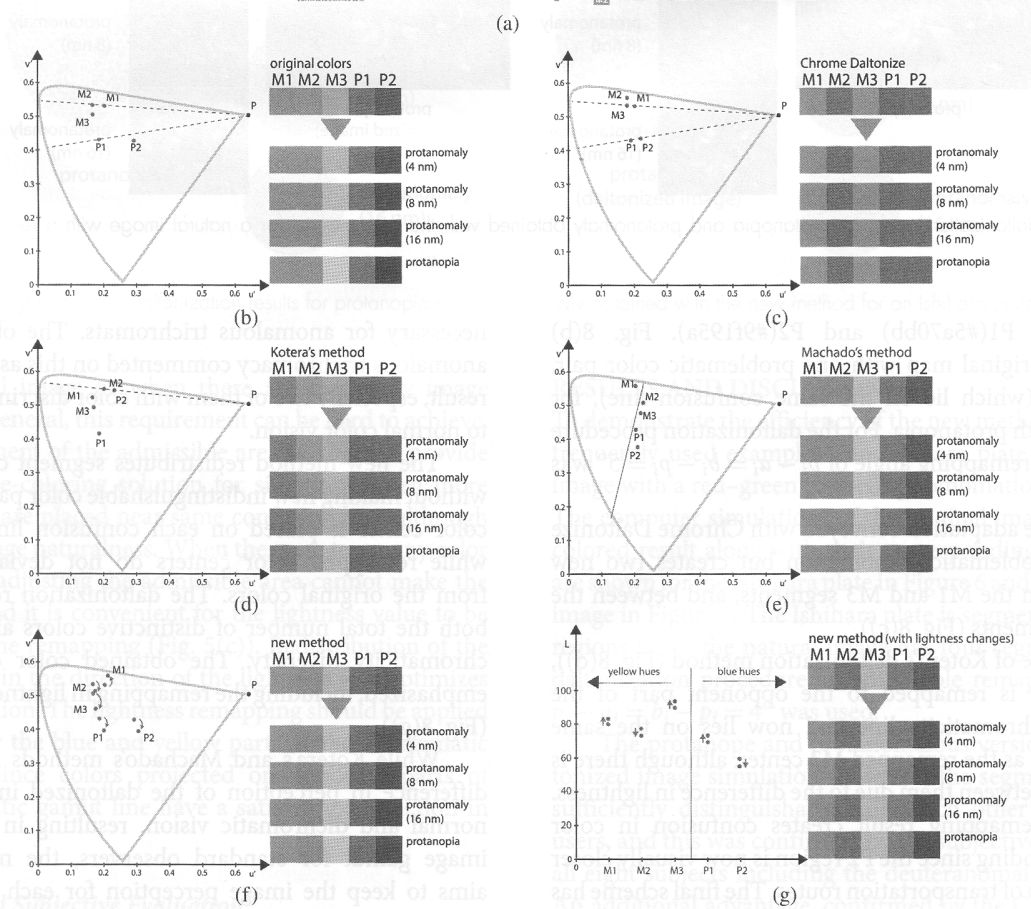
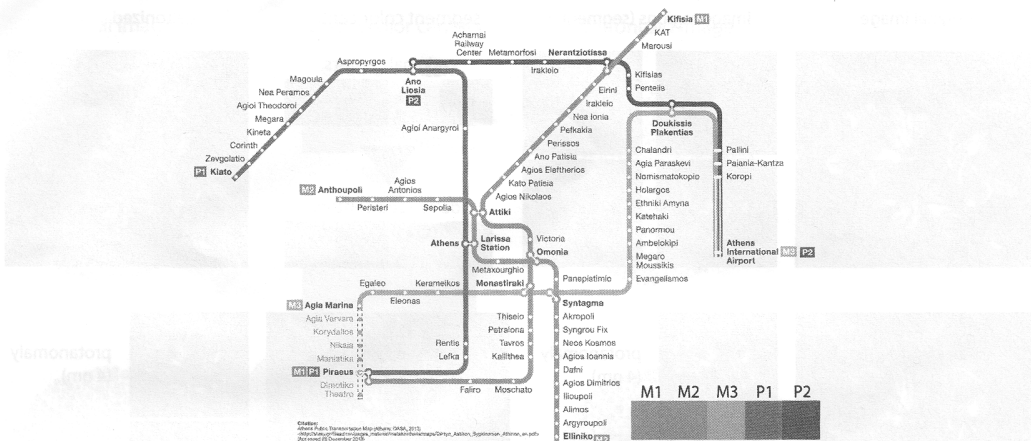


**Figure 8.** The daltonization results. (a) The original map with the color scheme. Protanopic and protanomalous simulation of color centers and their positions in the CIE  $u'v'$  chromaticity diagram for (b) the original color scheme, (c) the color scheme daltonized with Chrome Daltonize, (d) the color scheme daltonized with Kotera's method, (e) the color scheme daltonized with Machado's method, (f) the color scheme daltonized with the new method, (g) the color scheme daltonized with the new method including lightness remapping. (The red points are the positions of the original color centers and the blue points represent the new positions.)

red–green confusing combinations like the ones presented in Figs. 6 and 7. For the daltonization procedure an admissible remapping angle of  $p_i - a_i = b_i - p_i = 5^\circ$  was used and the number of segments was six. The remapped color centers stayed very close to the original positions since the original image had satisfying chromaticity redistribution.

Observers evaluated the perceived qualities of our daltonization result and the original image as similar, where

two of them (one protanope and one protanomalous subject) picked the daltonization result as a slightly better choice. All eight observers evaluated Machado's and Kotera's results (Fig. 9) as deterioration in color distinction and global diversity of chromaticity. This example shows that daltonization conveyed with the proposed naturalness-preserving method does not lead to deterioration in image quality





Figure 9. The daltonization results for protanopia and protanomaly obtained with Machado's, Kotera's and the new method for a complex natural image with large color gamut.

regardless of the content complexity. By increasing the initial image gamut, the daltonization result will be closer to the original image.

## CONCLUSIONS

Since the use of color to convey visual information in multimedia content has increased, it has become more justified to tackle the accessibility of color information for the color deficient population. Objective computer simulation results for the proposed daltonization, verified with the evaluations of eight CVD users, show an increased number of distinctive hues that a CVD observer can perceive in image content, without the possibility of creating new problematic color combinations between image segments. The proposed method is appropriate for all dichromatic and anomalous trichromatic CVD and seeks equilibrium between increased color distinction and preserved naturalness in a computationally simple way. It overcomes both the color differentiation limitation of content-independent methods and the naturalness-preserving problem of content-dependent methods optimized for dichromats. The full potential of this method is reachable in the digital environment where exact parameters concerning the type and severity of the deficiency can provide the optimal result for every CVD individual separately with personalized daltonization.

Although this article focuses on the concept and method of remapping, further investigation on segmentation issues may give solutions for application in the real time environment.

## ACKNOWLEDGMENT

This work was supported by the Serbian Ministry of Science and Technological Development, Grant No.: 35027 'The development of software model for improvement of knowledge and production in graphic arts industry'.

## REFERENCES

- 1 M. Fairchild, *Color Appearance Models* (John Wiley & Sons, Chichester, 2005), 9 p.
- 2 C. Rigden, "The eye of the beholder—designing for colour-blind users," *Br. Telecommun. Eng.* 17, 2–6 (1999).
- 3 G. M. Machado, M. M. Oliveira, and L. A. F. Fernandes, "A physiologically—based model for simulation of color vision deficiency," *IEEE Trans. Vis. Comput. Graphics* 15, 1291–1298 (2009).
- 4 G. Sharma, *Digital Color Imaging* (CRC Press, London, 2003).
- 5 J. Mollon and B. C. Regan, *Cambridge Colour Test* (Cambridge Research Systems, Cambridge, 2000).
- 6 H. Brettel, F. Vienot, and J. Mollon, "Computerized simulation of color appearance for dichromats," *J. Opt. Soc. Am.* 14, 2647–2655 (1997).
- 7 F. Vienot, H. Brettel, and J. Mollon, "Digital video colourmaps for checking the legibility of displays by dichromats," *Color Res. Appl.* 24, 243–252 (1999).
- 8 F. Vienot, H. Brettel, L. Ott, A. Ben M'Barek, and J. Mollon, "What do colour-blind people see?," *Nature* 376, 127–128 (1995).
- 9 Vischeck. Available at: <http://www.vischeck.com>.
- 10 Visolve. Available at: <http://www.ryobi-sol.co.jp/visolve/en/>.
- 11 Chrome Daltonize extension. Available at: <https://chrome.google.com/webstore/detail/chrome-daltonize/efeladnkafmoofnbgdbfaieabmejfcf>.
- 12 Colour-blindness filters, Adobe InDesign CS6. Available at: <http://www.adobe.com/accessibility.html>.
- 13 N. Ohta and R. Robertson, *Colorimetry: Fundamentals and Applications* (John Wiley & Sons, Chichester, 2005), 115 p.
- 14 J. Walraven and J. W. A. M. Alferdinck, "Color displays for the color blind," *Proc. IS&T/SID 5th Color Imaging Conf. (IS&T, Springfield, VA, 1997)*, pp. 17–23.

- 15 P. Capilla, M. A. Díez-Ajenjo, M. J. Luque, P. Capilla, M. A. Díez-Ajenjo, M. J. Luque, and J. Malo, "Corresponding-pair procedure: a new approach to simulation of dichromatic color perception," *J. Opt. Soc. Am.* **12**, 176–86 (2004).
- 16 Web Contents Accessibility Guidelines. Available at: [www.w3.org/TR/WCAG20](http://www.w3.org/TR/WCAG20).
- 17 Techniques for Web Content Accessibility. Available at: [www.w3.org/TR/WCAG-TECHS](http://www.w3.org/TR/WCAG-TECHS).
- 18 Web Content Tool Consortium. Available at: [www.wat-c.org](http://www.wat-c.org).
- 19 J. Ruminski, M. Bajorek, J. Ruminska, J. Wtorek, and A. Bujnowski, "Colour transformation methods for dichromats," *Proc. 3rd Human System Interactions* (Rzeszow, Poland, 2010), pp. 453–470.
- 20 J. Huang, Y. C. Tseng, S. I. Wu, and S. J. Wang, "Information preserving color transformation for protanopia and deuteranopia," *IEEE Signal Process. Lett.* **14**, 711–714 (2007).
- 21 G. Iaccarino, D. Malandrino, M. D. Percio, and V. Scarano, "Efficient edge-services for colorblind users," *WWW'06. Proc.* (Edinburgh, Scotland, 2006), pp. 9–10.
- 22 N. Milic and D. Novaković, "Development of plug-in for simulation of different types of colour vision deficiency and enhancement of the image for viewers with protanopia and deuteranopia," *Proc. PFD09 3rd Int. Student Conf. on Print and Media Technol.* (Chemnitz, Germany, 2009), pp. 315–322.
- 23 C. N. Anagnostopoulos, G. Tsekouras, I. Anagnostopoulos, and C. Kalloniatis, "Intelligent Modification for the daltonization process of digitized paintings," *Proc. ICVS 5th Int. Conf. on Computer Vision Systems* (Bielefeld, Germany, 2007), Available at: <http://biacoll.uni-bielefeld.de>.
- 24 P. Fidaner, L. Poliang, and N. Ozguven, "Analysis of color blindness," Available at: [http://scien.stanford.edu/pages/labsite/2005/psych221/projects/05/ofidaner/colorblindness\\_project.htm](http://scien.stanford.edu/pages/labsite/2005/psych221/projects/05/ofidaner/colorblindness_project.htm).
- 25 H. Kotera, "A study on spectral response for dichromatic vision," *Proc. IS&T/SID 19th Color and Imaging Conf.* (IS&T, Springfield, VA, 2011), pp. 8–13.
- 26 H. Kotera, "Optimal Daltonization by Spectral Shift for Dichromatic Vision," *Proc. IS&T/SID 20th Color and Imaging Conf.* (IS&T, Springfield, VA, 2012), pp. 302–308.
- 27 M. Ichikawa, K. Tanaka, S. Kondo, K. Hiroshima, K. Ichikawa, S. Tanabe, and K. Fukami, "Web-page color modification for barrier-free color vision with genetic algorithm," *LNCS 2724*, 2134–2146 (2003).
- 28 M. Ichikawa, K. Tanaka, S. Kondo, K. Hiroshima, K. Ichikawa, S. Tanabe, and K. Fukami, "Preliminary study on color modification for still images to realize barrier-free color vision," *Proc. SMC IEEE Int. Conf. Systems Man: Cybernetics* (Hague, Netherlands, 2004), pp. 36–41.
- 29 G. R. Kuhn, M. M. Oliveira, and L. A. F. Fernandes, "An efficient naturalness-preserving image-recoloring method for dichromats," *IEEE Trans. Vis. Comput. Graphics* **14**, 1747–1754 (2008).
- 30 K. Rasche, R. Geist, and J. Westall, "Detail preserving reproduction of color images for monochromats and dichromats," *IEEE Comput. Graph. Appl.* **25**, 22–30 (2005).
- 31 Y. Ma, X. Gu, and Y. Wang, "Color discrimination enhancement for dichromats using self-organizing colour transformation," *Inf. Sci.* **179**, 830–843 (2009).
- 32 J. Huang, S. Wu, and S. Chen, "Enhancing color representation for the color vision impaired," *Proc. ECCV Int. Workshop on Computer Vision Applications for the Visually Impaired in Conjunction with European Conf. on Computer Vision* (Marseille, France, 2008), Available at: [www.ski.org/Rehab/Coughlan\\_lab/General/CVAVI08pubs/EnhancingColor.pdf](http://www.ski.org/Rehab/Coughlan_lab/General/CVAVI08pubs/EnhancingColor.pdf).
- 33 G. M. Machado and M. M. Oliveira, "Real-time temporal-coherent color contrast enhancement for dichromats," *Comput. Graph. Forum* **29**, 933–942 (2010).
- 34 K-means segmentation, Matlab. Available at: <http://www.mathworks.com/help/images/examples/color-based-segmentation-using-k-means-clustering.html>.
- 35 M. E. Celebi, *Partitional Clustering Algorithms* (Springer, Shreveport, 2014).
- 36 D. MacAdam, "Visual sensitivities to color differences in daylight," *J. Opt. Soc. Am.* **32**, 247–274 (1942).